DOI: 10.1002/adem.200700015

Superlightweight Nanoengineered Aluminum for Strength under Impact**

By *Haitao Zhang, Jichun Ye, Shailendra P. Joshi, Julie M. Schoenung, Ernest S. C. Chin, George A. Gazonas,* and *Kaliat T. Ramesh**

The search for better armor materials is intimately tied to the history of mankind, and the rise and fall of civilizations is sometimes related to the development of new armor systems [1]. An ideal armor material is expected to have three attributes: sufficient strength at high impact velocities, sufficient toughness to carry normal structural loads, and low weight. The degree to which each attribute is desirable depends both on what is being protected (a vehicle or an individual) and on the specific threat (e.g. an anti-vehicle weapon or a bullet). Materials that have all three attributes have been extraordinarily difficult to find, and much current vehicular armor uses combinations of multiple materials, one of which carries the bulk of the structural load and another, which has the appropriate impact response. Constructing such "armor packages" with sufficiently low weight often defines the limits of vehicular weight, leading directly to limits on the ability to rapidly project military power and constraints on geopolitical operations during global conflicts.

Materials used for armor have evolved from natural sources such as wood and leather to synthetics that include fibers, monolithics and hybrid composites of metals, ceramics and polymers. Recent advances in armor materials include aramid fibers for ballistic vests and boron carbide for small arms protective inserts (SAPI) plates. In a monolithic armor design, the material is modified to attain a balanced range of properties to prevent penetration and fragmentation. This is a typical compromise between hardness and ductility in most materials. In modern armor designs, discrete layers of materials are functionally optimized to sequentially shatter/erode the projectile followed by containing all residual debris. This strategy maximizes the gains from each contributing component. However, the performance of such an armor system is bounded by the weighted average of the macro-components in the armor recipe. In this paper, a selectively dispersed nano/micro component material (TriMod) is demonstrated to exhibit extraordinary dynamic flow strength that far exceeds any of the respective individual constituents. This watershed innovation has created a new path to design native armor materials with properties exceeding that of layered armor designs, without compromises.

Aluminum (Al) alloys are the most widely used metals in technologies where weight reduction is a major design consideration, and specific approaches such as solid solution strengthening and age-hardening[2] have been developed to strengthen Al-based materials. However, the total strength that is attainable with these approaches is relatively small, and the best traditional aluminum armor materials (such as Al-5083, with 4.4 wt.% Mg, 0.7 wt.% Mn, and 0.15 wt.% Cr and the balance Al) do not have significant advantages over the better armor steels (Fig. 1). We describe here a nanoengineered aluminum-based material that has remarkable properties relevant to armor systems. The material achieves dramatic mechanical properties at impact rates of deformation through a combination of three micro-structural length scale approaches: strengthening through a nanocrystalline core architecture, additional strengthening through length-scale de-

[*] *Dr. H. Zhang,* Dr. S. P. Joshi, Prof. K. T. Ramesh*
Department of Mechanical Engineering
The Johns Hopkins University
Baltimore, MD 21218 USA
Email: ramesh@jhu.edu
Dr. J. Ye, Prof. J. M. Schoenung
Department of Chemical Engineering and Materials Science
University of California, Davis
Davis, CA 95616 USA
Phone: (530) 752-5840
Email: jmschoenung@ucdavis.edu
Dr. E. S. C. Chin, Dr. G. A. Gazonas
U.S. Army Research Laboratory
Weapons and Materials Research Directorate
Aberdeen Proving Ground, MD 21005 USA
**now Postdoctoral Fellow*
Aerospace Engineering and Engineering Mechanics
The University of Texas at Austin
210 E. 24th Street, WRW 110B
1 University Station, C0600, Austin, TX 78712-0235

[**] *This work was performed under the auspices of the Center for Advanced Metallic and Ceramic Systems (CAMCS) at the Johns Hopkins University and supported by the US Army Research Laboratory through ARMAC-RTP Cooperative Agreement No. DAAD19-01-2-0003. SPJ and KTR also acknowledge the financial support provided by the Army Research Laboratory through ARMAC-RTP Cooperative Agreement No. W911NF-06-2-0006. JY and JMS gratefully acknowledge support from the Office of Naval Research under contract No. N00014-03-C-0163.*

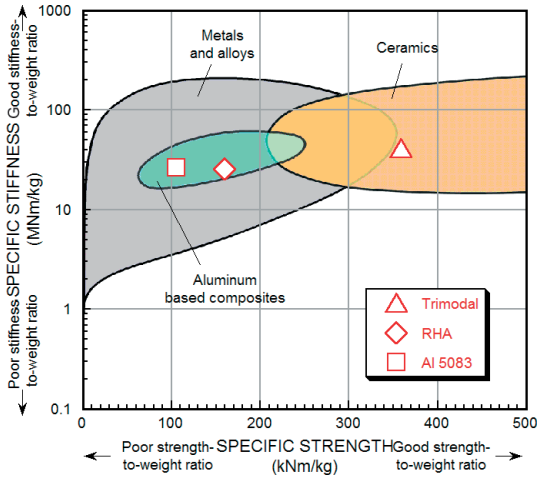

Fig. 1. Plot of the specific stiffness versus specific strength of various materials. The substantial improvement in specific strength of the nanoengineered tri-modal composite aluminum alloy in comparison to the most common armor steel (Rolled Homogeneous Armor or RHA) is apparent. This new material has specific strength properties comparable to ceramics, while retaining substantial ductility. (http://www-materials.eng.cam.ac.uk/mpsite/interactive_charts/)

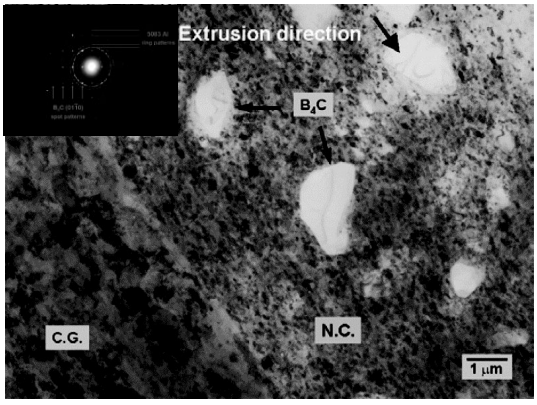

Fig. 2. Transmission electron micrograph showing nanocrystalline (nc) aluminum (nc-Al) matrix containing micron sized boron carbide particles, with this nc composite embedded within a coarse-grained microcrystalline aluminum (CG) matrix. The selected area diffraction pattern that was taken from the B_4C/nc-Al interface is composed of ring patterns (from nc-Al) and spots pattern (from B_4C). High temperature phases were not detected in this diffraction pattern, indicating a clean B_4C/NC Al interface developed after cryomilling and consolidation.

pendent reinforcement with micron-size ceramic particles, and enhanced ductility through the incorporation of a certain volume fraction of microscale grains. The resulting "tri-modal" aluminum-based material has substantial ductility while achieving extraordinary specific strengths under very high rates of deformation, and shows great promise in armor applications.

The processes used to synthesize this material are described in detail elsewhere (also see methods section).[3] Fundamentally, a nanocrystalline 5083 aluminum composite powder is first produced by cryomilling 5083 aluminum powders with boron carbide ceramic particulates. This nanocomposite powder is then degassed and blended with microscale 5083 aluminum. This "tri-modal" composite powder is then consolidated with conventional powder metallurgy techniques such as cold isostatic pressing plus extrusion to generate a bulk tri-modal composite aluminum-based material.

The tri-modal Al-5083 composite alloy possesses higher stiffness and extraordinary strength in comparison to the conventional Al-5083 alloy. A measure of the remarkable nature of this material is shown in Figure 1, which presents the specific stiffness (ratio of Young's modulus to density) of materials as a function of the specific strength (ratio of yield strength to density). The new material has specific strength properties that are a dramatic improvement over Rolled Homogeneous Armor (RHA) steel, and is in fact comparable to ceramics in this respect while retaining some of the beneficial ductility associated with metallic alloys.

The microstructure of this novel material is shown in the transmission electron micrograph of Figure 2. The micrograph shows a nanocrystalline aluminum matrix containing micron-sized boron carbide particles, with this nanocrystalline composite itself embedded in a "coarse-grained" (CG) or microcrystalline aluminum material. Both the nanocrystalline and microcrystalline aluminum materials have the 5083 aluminum composition, albeit modified by the cryomilling process. The resulting tri-modal composite has truly remarkable mechanical properties as shown next.

High Strain Rate Mechanical Properties

This aluminum-based material exhibits a very high strength (950–1000 MPa) when loaded at high strain rates. Figure 3 presents stress vs. strain curves obtained on this material at strain rates of 3200 s^{-1} and 11,000 s^{-1} using compression Kolsky bar (see methods section). Strength levels of this

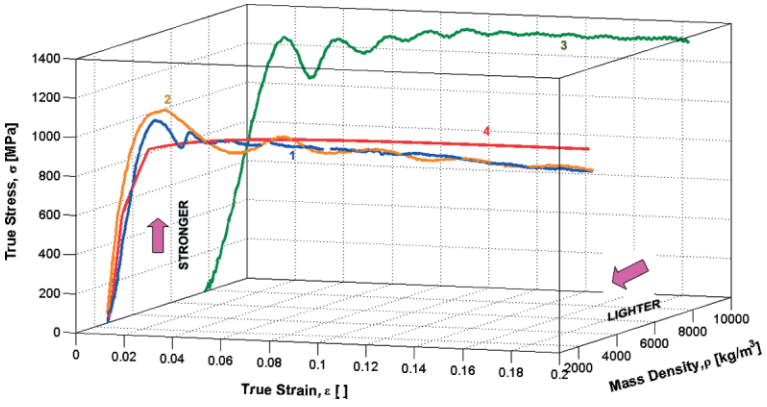

Fig. 3. Mechanical behavior of nanoengineered tri-modal composite aluminum alloy at high compressive strain rates of 3200 s^{-1} (Curve 1) and 11000 s^{-1} (Curve 2). Curve 3 shows the mechanical response of current armor steel (RHA) at 4200 s^{-1}; the steel is nearly 3 times as dense as the aluminum alloy. Curve 4 is the prediction of the model presented in this paper. The tri-modal material has remarkable strength and substantial plastic deformation at these impact rates. The oscillations in the experimental curves are a result of experimental configuration and do not represent the material behavior.

ADVANCED ENGINEERING MATERIALS

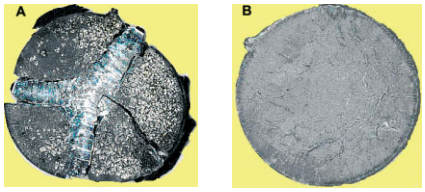

Fig. 4. Photographs of nanoengineered tri-modal composite aluminum samples after deformation at high strain rates. (a) Deformation at a strain rate of 3200 s^{-1} and (b) a higher strain rate of 11050 s^{-1}. Note the dramatic change in the heterogeneity of the deformation at the higher strain rate.

magnitude are truly remarkable for an aluminum-based material and have never been observed before for such materials at these strain rates. The mechanical response of the most common current armor steel (RHA) measured at similar strain rates is also shown in the figure – we note that this steel is nearly three times as dense as the aluminum alloy.

What is even more remarkable is that these samples exhibit strains to failure of more than 20 % in these high strain rate compressive tests, and the strain to failure appears to increase with strain rate. Figure 4 shows two specimens that have been recovered after high strain rate compression tests: the first from a test with a medium strain rate of 3200 s^{-1} (Fig. 4(a)) and the second from a test with a higher strain rate of 11050 s^{-1} (Fig. 4(b)).

The specimen in Figure 4(a) shows major shear failures, oriented at approximately 45 degrees to the compression axis, leading eventually to failure of the sample (albeit at macroscopic strains much larger than observed in quasistatic experiments on nanocrystalline metals). The specimen in Figure 4(b) does not show such major cracks, even with a much larger total strain (0.56 as measured by the circumferential expansion). Instead, large numbers of micro-cracks are apparent on the specimen surfaces in Figure 4(b). This indicates a rate-dependent damage evolution process in the material, with much greater nucleation of the microcracks at the high strain rates but insufficient time for coalescence of the cracks (which leads to the macroscopic failure at lower strain rates). Under low rate deformation, a single or several major cracks are nucleated (the weakest defect being triggered first); these grow and suppress the nucleation of additional cracks, but their rapid growth results in catastrophic failure of the specimen.[4] The increased nucleation of microcracks at high rates of deformation leads to an effective increase in the total strain to failure at high strain rates. Microcracks are typically nucleated in regions of NC Al and B_4C particles, but are likely to be stopped or decelerated by the dislocation activity in the CG Al.

Length-Scale Dependent Micromechanical Modeling

A model that quantitatively describes the underlying physics of the exceptional mechanical behavior of the composite has been developed and will be discussed in detail elsewhere [5]. The features of this strength model are essentially independent of strain rate, and we do not seek to capture the variation of the strain to failure with strain rate, or the rate-dependent nucleation and growth of microcracks (such behaviors are described by a failure model). Mechanical milling, consolidation and temperature lead to a peculiar microstructure that derives its strength from four specific strengthening mechanisms, in addition to the normal load transfer characteristics of the composite.[6–8] These are: (1) grain boundary strengthening through grain size refinement, (2) particle-size strengthening through the ceramic reinforcement, (3) dispersoid strengthening and (4) work hardening due to the prior plastic work from cryomilling and extrusion. With regard to the first mechanism, the grain size refinement of the Al-5083 leads to an initially stronger matrix than a conventional coarse-grained matrix of the same material. This is the well-known *Hall-Petch* effect, and the yield strength scales inversely with square root of the grain size.[9,10] The second mechanism is due to the addition of micron-sized ceramic particles to this nanostructured Al-5083. As in any particulate composite of this type, the particles act as reinforcement in enhancing the stiffness as well as the strength of the matrix by sharing a significant portion of the applied load. In addition, thermo-elastic mismatch between the particles and the matrix gives rise to geometrically necessary dislocations (GNDs),[11] the GND density is inversely proportional to the particle size. The GNDs generated at the matrix-particle interfaces relieve the matrix of high stresses (the *dislocation punching* mechanism[12]), resulting in lower stresses in the matrix and therefore increased strength. The third strengthening mechanism is the presence of dispersoids (produced during the cryomilling phase) that are distributed in the matrix, and this also plays a role in strengthening. The strengthening effect of the dispersoids can be explained by the *Orowan bowing* mechanism.[13] A fourth contribution to strengthening is the prior plastic work done by cryomilling and extrusion that may cause the material to work-harden.[14]

We have constructed a quantitative model based on Mori-Tanaka method[5,15] accounting for the direct strengthening through load transfer between the ceramic reinforcement and the matrix and the length-scale effects. The analysis is broken down into two stages, representing the hierarchical nature of the material: a first stage describing the nanocomposite with particulate inclusions, and a second stage describing the nano-micro composite corresponding to the blend of the coarse-grained and nanocomposite components. The stage-I analysis accounts for grain size, dislocation punching and Orowan mechanisms present in the particle reinforced ultrafine grained (UFG) composite; the stage-II analysis takes the stage-I response as input and combines the response of CG phase (accounting for the grain size of the CG phase), resulting in the overall composite response. Specific parameters for the model are derived from independent experiments and microstructural characterization.[3,16,17]

Figure 3 also shows the response predicted by the model and demonstrates good prediction of the measured response. Note that traditional pure continuum models cannot predict

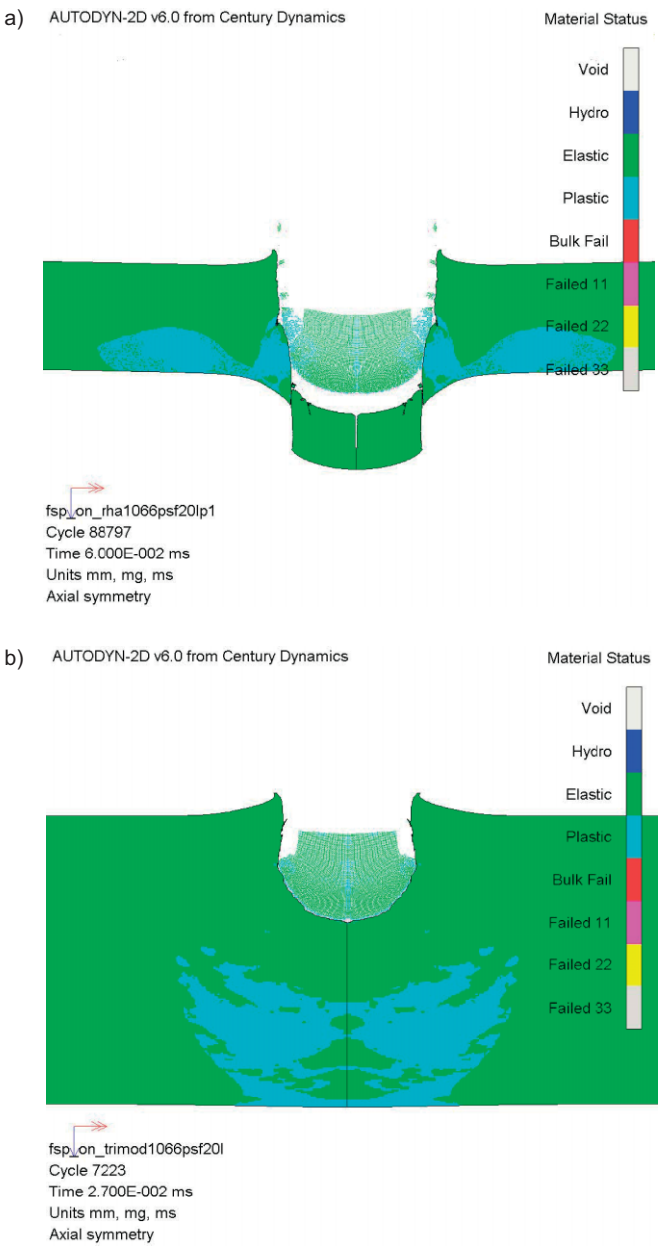

Fig. 5. (a) Perforation of a 20 psf RHA target by a 0.50 cal FSP traveling at 1.066 km/s at 60 μs. (b) Penetration of a 20 psf tri-modal composite aluminum alloy target by a 0.50 cal FSP traveling at 1.066 km/s at 27 μs.

the observed response without specifically handling the length-scale dependent features of the first three strengthening mechanisms, as does the model presented here. The great advantage of successfully modeling the behavior is that we now have guidelines that can be used to optimize the behavior of the material behavior at high strain rates with respect to specific functions.

Impact Simulations

It is difficult to define validated metrics that immediately rank materials as good or better armor materials, because of the complexity of the impact loading problem associated with the armor/anti-armor problem and because of the variety of threats that can be encountered. The best current approach (other than full-scale testing) to evaluate the potential of new materials for armor applications is through full armor-level computational simulations of a terminal ballistic event. We present such simulations in this section.

We present the results of impact and penetration response of trimodal composite aluminum alloy (ρ = 2.68 g/cm^3) and RHA targets (ρ = 7.83 g/cm^3) by high-velocity mild-steel fragments (Rockwell C-30). Using AUTODYN,[18] a 2-D axisymmetric analysis of the fragment simulating projectile (FSP) and both the targets is carried out. Equal areal density targets are assumed. The results of the simulations for the 0.50 caliber (0.5 cal) FSP perforation of a 20 pounds per square foot (psf) RHA target are illustrated in Figure 5(a) at a velocity of 1.066 km/s. Interestingly, it appears the RHA target has failed by plugging through adiabatic shear without explicit use of a shear-band model. The effectiveness of an equivalent areal density target consisting of the tri-modal material is depicted in Figure 5(b), which illustrates the predicted FSP penetration depth (only one-third the target thickness) for the same velocity at which the RHA fails. The simulations indicate that the tri-modal material may have the potential for dramatic improvement in the degree of protection offered against FSPs (for the same weight of armor); although we have a limited knowledge of the dynamic failure mechanisms active in the tri-modal material. A natural question is: what impact velocity is needed to completely perforate a 20 psf target consisting of this tri-modal material? With the limited constitutive and failure behavior compiled thus far, this question can best be answered by conducting carefully controlled ballistic tests.

In summary, we demonstrate that the hierarchical nanoengineered aluminum-based material derives superhigh strengths through microstructural length scale effects. At the high strain rates associated with impact loading, the new material exhibits large strains to failure indicating a rate dependent failure process. The juxtaposition of strength and high failure strains, at one-third the specific weight of steels suggests dramatic possibilities for improved, energy efficient structural systems for impact.

Materials and Methods

A form of mechanical milling called cryomilling (i.e., mechanical milling in liquid nitrogen) can fabricate Al-based materials with uniformity of reinforcement, strong interface between reinforcement/matrix, and a nc Al-based matrix.[3] In addition, the dispersoids formed during cryomilling, such as oxides and nitrides, contribute to the thermal stability[19] and strength[20] of the bulk, consolidated nc Al-based material. Furthermore, coarse-grained Al alloy powder can be combined with the cryomilled nanocomposite powder to improve the ductility of the bulk, consolidated material.[21,22]

In the present work, an equiaxed nanocomposite powder with particulate B_4C reinforcement uniformly distributed in

the nc (~ 25 nm) 5083 Al was fabricated using cryomilling.[3] B_4C was selected as the reinforcement due to its high specific strength, specific toughness and high impact resistance. Moreover, it is even lighter than the Al alloy, resulting in a lighter material by introducing it into the 5083 Al matrix. A process control agent was added during the cryomilling step in order to improve powder yield. The cryomilled nanocomposite powder was degassed and then blended with conventional gas-atomized coarse-grained 5083 Al powder. The bulk consolidated tri-modal composite material was prepared by using conventional powder metallurgy methods such as cold isostatic pressing and extrusion.

Microscopic investigation of the cryomilled powder shows that the nanocomposite powder has a homogeneous distribution in the reinforcement, a strong interface between the reinforcement and the matrix, and a nc Al matrix.[16,17] Investigation of the bulk, consolidated material shows regions of nc matrix (100-200 nm grain size) with boron carbide embedded within, and coarse-grained regions (500-1000 nm) that result from the addition of unmilled powder. After extrusion, both the coarse-grained metallic regions and the nanocomposite regions are elongated and are alternately stacked along the extrusion direction (Fig. 2 in the main article), acting like "whiskers", which is an effective geometric configuration for more effective load transfer. High temperature phases, which would be detrimental to mechanical behavior, were not detected at the interface between the nc matrix and the boron carbide reinforcement, even after consolidation. This microstructure indicates that the load can be transferred from the coarse-grained regions to the nc regions of the matrix (because of their identical chemical composition), and then from the nc regions to the hard B_4C particle reinforcement (because of the strong, clean interface).

Mechanical Testing Methods

Compression Kolsky bar (or split-Hopkinson pressure bar)[23] tests were conducted to obtain high strain rate compressive response of the materials over a strain rate range of 10^3 to 10^4 s^{-1}. The specimens were 5 mm in diameter with a length-to-diameter ratio of 0.6 in accordance with standard practice for metallic specimens in the Kolsky bar technique.

Received: January 17, 2007
Final version: January 27, 2007

[1] J. Diamond, *Guns, Germs and Steel: The Fates of Human Soc.* 1999, W.W. NORTON & COMPANY.
[2] G. E. Totten, M. D. Scott, *Handbook of Aluminum*, New York: Marcel Dekker, Inc. **2003**.
[3] J. Ye, B. Q. Han, Z. Lee, B. Ahn, S. R. Nutt, J. M. Schoenung, *Scr. Mater.* **2005**, *53*, 481.
[4] B. Paliwal, K. T. Ramesh, J. McCauley, *J. Am. Ceram. Soc.* **2006**, *89*, 2128.
[5] S. P. Joshi, K. T. Ramesh, *In Preparation* **2007**.
[6] N. A. Fleck, G. M. Muller, M. F. Ashby, J. W. Hutchinson, *Acta Metall. Mater.* **1994**, *42*, 475.
[7] D. J. Lloyd, *Int. Mater. Rev.* **1994**, *39*, 1.
[8] Z. Xue, Y. Huang, M. Li, *Acta Mater.* **2002**, *50*, 149.
[9] E. O. Hall, *Proc. R. Phys. London, B.* **1951**, *64*, 747.
[10] N. J. Petch, *J. Iron Steel Inst.* **1953**, *174*, 25.
[11] M. F. Ashby, *Philos. Mag.* **1970**, *21*, 399.
[12] R. J. Arsenault, N. Shi, *Mater. Sci. Eng. A.* **1986**, *81*, 175.
[13] B. Q. Han, Z. Lee, S. R. Nutt, E. J. Lavernia, F. A. Mohammed, *Metall. Mater. Trans. A.* **2003**, *34A*, 603.
[14] D. B. Witkin, E. J. Lavernia, *Prog. Mater. Sci.* **2005**, *51*, 1.
[15] S. P. Joshi, K. T. Ramesh, B. Q. Han, E. J. Lavernia, *Metall. Mater. Trans. A.* **2006**, *37A*, 2397.
[16] J. Ye, J. He, J. M. Schoenung, *Metall. Mater. Trans. A.* **2006**, *37*, 3099.
[17] J. Ye, Z. Lee, B. Ahn, J. He, S. R. Nutt, J. M. Schoenung, *Metall. Mater. Trans. A.* **2006**, *37*, 3111.
[18] *Autodyn Theory Manual.* 2004, ANSYS, Inc.
[19] F. Zhou, J. Lee, S. Dallek, E. J. Lavernia, *J. Mater. Res.* **2001**, *16*, 3451.
[20] L. M. Brown, R. K. Ham, in *Strengthening Meth. in Cryst.* ELSEVIER. **1971**. 9.
[21] Y. Wang, M. Chen, F. Zhou, E. Ma, *Nature* **2002**, *419*, 912.
[22] D. Witkin, L. Z. R. Rodriguez, S. R. Nutt, E. J. Lavernia, *Scr. Mater.* **2003**, *49*, 297.
[23] H. Kolsky, *Proc. R. Phys. London B* **1949**, *62*, 676.

